Article:
Wildes, A.R. and Cowlam, N. (2011) Sperimagnetism in Fe(78)Er(5)B(17) and Fe(64)Er(19)B(17) metallic glasses: I. Moment values and non-collinear components. Journal of Physics: Condensed Matter, 23 (49). Art no. 496004. ISSN: 0953-8984

https://doi.org/10.1088/0953-8984/23/49/496004

Sperimagnetism in $Fe_{78}Er_5B_{17}$ and $Fe_{64}Er_{19}B_{17}$ metallic glasses. I –Moment values and non-collinear components.

A R Wildes[a] and N Cowlam[b]

[a]Institut Laue-Langevin, BP 156, 6 rue jules Horowitz, 38042 GRENOBLE Cedex 9, France,

[b]Department of Physics and Astronomy, University of Sheffield, SHEFFIELD, S3 7RH, U.K,

Abstract.

Magnetisation measurements have been made on a $Fe_{64}Er_{19}B_{17}$ glass, which exhibits ferrimagnetic compensation at T_{comp} = 112K and polarised beam neutron scattering measurements have been made on $Fe_{78}Er_5B_{17}$ and $Fe_{64}Er_{19}B_{17}$ glasses to supplement the measurements made earlier on $Fe_{64}Er_{19}B_{17}$. The magnetisation data were analysed with a phenomenological model, to find the magnetic moments and their components needed to interpret the neutron data. Four spin-dependent scattering cross-sections were obtained in absolute units from each neutron experiment, to determine the atomic-scale magnetic structures of the two glasses. The finite spin-flip cross-sections confirmed that these $(Fe,Er)_{83}B_{17}$ glasses are non-collinear ferrimagnets. The cross-sections were calculated using a model based on random cone arrangements of the magnetic moments. The moment values and the random cone angles were refined in the calculations, which produced good agreement between the calculated curves and the experimental data. The forward limit of the spin-flip cross-sections $\left|\partial\sigma^{\pm\mp}/\partial\Omega\right|_{Q=0}$ of the $Fe_{64}Er_{19}B_{17}$ glass which peaked at T_{comp} and the temperature variation of the total scattering amplitudes $\left(b \mp p^{\parallel}(Q)\right)$ suggested that the random cone angles open fully so that the collinear components $p^{\parallel}(Q)$ tend to zero at T_{comp}. The ferrimagnetic compensation is therefore characterised by an equality of the magnetic sublattices; the reversal of the magnetic structure and a compensated sperimagnetic phase which appears at T_{comp}.

1.0) Introduction

The presence of collinear and non-collinear magnetic structures in metallic glasses can be established by using polarised beam neutron scattering. Four spin-dependent scattering cross-sections are measured in a typical experiment with one dimensional polarisation analysis, (see Figure 1 of [1]) They are conventionally divided into two non spin-flip cross-sections, for which the neutron polarisation is unchanged on scattering and two spin-flip cross-sections for which it is rotated by 180º or 'flipped' on scattering. These cross-sections provide direct information about the collinear and the non-collinear components of the magnetic moments respectively.

Many of the transition metal – metalloid ($TM_{83}met_{17}$-type) glasses are non-collinear ferromagnets [1] and the introduction of rare earth (RE) ions to these has the potential to change their magnetic structures significantly. The magnetic structures in binary, amorphous rare earth – transition metal (RE-TM) alloys are usually described in terms of a non-collinear RE sublattice immersed in a ferromagnetic matrix [2, 3]. These non-collinear structures arise because the large spin-orbit coupling at the RE sites leads to large local anisotropies which compete with the exchange interactions.

Rather surprisingly, $(Fe,Tb)_{83}B_{17}$ glasses have been found to be *collinear* ferrimagnets by polarised beam neutron scattering [4]. The substitution of the large RE ion with its equally large magnetic moment was found to change the form and shape of the measured non spin-flip cross-sections significantly in comparison with those of the parental $TM_{83}met_{17}$ glasses [1]. These non spin-flip cross-sections of the $(Fe,Tb)_{83}B_{17}$ glasses were nevertheless successfully simulated, by using a combination of known and derived partial structure factors [4]. Magnetisation, Mössbauer spectroscopy and X-ray magnetic circular dichroism (XMCD) measurements on (Fe,Er)BSi glasses [5]; amorphous FeEr alloys [6, 7, 8] and a single $Fe_{66}Er_{19}B_{15}$ glass [9], suggest that $(Fe,Er)_{83}B_{17}$ are *non-collinear* ferrimagnets. They have been described by a sperimagnetic structure [10] in which the magnetic moments on the iron atoms point in a random cone that is ferrimagnetically coupled to a random cone of erbium moments. The identification of $\overline{\mu}_{Er}^{\parallel} = 8.0\mu_B$ in (Fe,Er)BSi glasses, (which is smaller than the absolute value $|\mu_{Er}| = 9.0\mu_B$), was originally interpreted as evidence that the erbium moments lay randomly on a cone with a fixed semi-vertex angle $\theta_{Er} = \cos^{-1}(8/9) = 27°$ to the applied field [5]. Such "empty cone" structures occur in some crystalline oxides [*e.g.* 11] because of fixed, competing exchange interactions. The alternative suggestion, that the

moments point randomly, at *every* angle to the applied field within a "filled cone" [9], is intuitively more consistent with the *range* of local environments that occurs in a glassy state. The semi-vertex angle of the cone will also change with temperature according to the relative magnitudes of the competing exchange interactions.

The (Fe,Er) – based glasses also exhibit ferrimagnetic compensation as a function of composition [5, 6] and temperature [6, 9]. We therefore made a preliminary study of a $Fe_{64}Er_{19}B_{17}$ glass at three different temperatures using polarised beam neutron scattering. The finite spin-flip cross-sections which were obtained, confirmed the presence of a non-collinear state [12].

The average components of the magnetic moments $\overline{\mu}^{\parallel}, \overline{\mu}^{\perp}$, parallel and perpendicular to the magnetic field are needed to describe the non spin-flip and spin-flip cross-sections, so that their values must be known as a function of composition and temperature. Magnetisation measurements relate to the mean collinear component of the moments

$$\overline{\mu}^{\parallel}{}_{meas} = \overline{\mu}^{\parallel}_{Er} - \overline{\mu}^{\parallel}_{Fe}.$$

They have been analysed in the past by first choosing a value of $\overline{\mu}^{\parallel}{}_{Fe}$ appropriate to *small concentrations*, to obtain $\overline{\mu}^{\parallel}_{Er}$ and then using this $\overline{\mu}^{\parallel}_{Er}$ to deduce $\overline{\mu}^{\parallel}{}_{Fe}$ for *all* compositions, - on the basis that $\overline{\mu}^{\parallel}_{Er}$ is independent of composition [5, 6]. It is not clear if this is completely justified when the erbium concentration is high and closer to the point where the ferrimagnetism is suppressed. In addition, there will be many different choices of the values of the total moments μ_{Fe}, μ_{Er} and the semi-vertex angles θ_{Fe}, θ_{Er} of their random cones in a non-collinear structure, which will lead to similar values of the $\overline{\mu}^{\parallel}$ and $\overline{\mu}^{\perp}$ components. It is finding the ***unique*** choice of the $\overline{\mu}^{\parallel}$, $\overline{\mu}^{\perp}$ components which makes the analysis of the data on the $(Fe,Er)_{83}B_{17}$ glasses more difficult than that of $(Fe,Tb)_{83}B_{17}$ [4]. The aim of the present work has been to obtain magnetic moment values from magnetisation data on our own $Fe_{64}Er_{19}B_{17}$ glass, which could be used confidently in the analysis of the neutron scattering. The neutron studies have also been extended to include a second series of measurements on a $Fe_{78}Er_5B_{17}$ glass at 2K and on the $Fe_{64}Er_{19}B_{17}$ glass at 100K, 112K, 125K and 180K.

The magnetisation data and its analysis using a phenomenological model, will be presented in Section 2 of this paper. Section 3 will cover the analysis of the spin-flip cross-sections and involve a refinement of the magnetic moment values already obtained. This provides direct evidence of the presence of the non-collinear state and its variation close to the compensation temperature T_{comp}. The analysis of the non spin-flip cross-sections will be covered separately

in **Part II** of this work, to avoid a paper of excessive length. It will involve a Fourier transform of the scattering data, relying solely on the values of the magnetic moments obtained in **Part I.** It will provide a coherent description of the atomic-scale structures in the two $(Fe,Er)_{83}B_{17}$ glasses.

1.1) Sample preparation and the experimental methods.

The preparation of the $Fe_{78}Er_5B_{17}$ and $Fe_{64}Er_{19}B_{17}$ glass ribbon by the chill-block melt spinning method has been explained previously [10]. A quantity of 0.16g of $Fe_{64}Er_{19}B_{17}$ glass ribbon was taken from the existing sample for the magnetisation measurements, which were made using an Oxford Instruments Vibrating Sample Magnetometer (VSM). The sample was mounted in a plexiglass cylinder on a conventional sample stick. Four runs were made, with H = 1.0T and H = 2.0T over 3K < T < 199K and then H = 0.5T over 3K< T < 296K, plus H = 0.1T over the same temperature range, with the sample cooled in zero field (ZFC). These temperature ranges covered the ferrimagnetic compensation temperature of the sample at $T_{comp} \approx$ 112K, but not the ferrimagnetic Néel temperature, expected to be around $T_{fN} \approx$ 350K, because of an upper limit on the operating temperature of the VSM. The data were obtained in units of Am^2kg^{-1} *versus* K and converted to magnetic moment per atom *versus* K, using the atomic number density of the glass 8.68×10^{24} atoms kg^{-1} and the equality $1\mu_B = 9.274\times10^{-24}Am^2$.

The second series of neutron experiments was made at the IN20 spectrometer at the Institute Laue-Langevin, using a cryomagnet with a vertical magnetic field. The $Fe_{64}Er_{19}B_{17}$ glass was measured inside an aluminium can at 100K, 112K and 125K (all in a field of 2T), to study the changes in magnetic structure which occur at the ferromagnetic compensation temperature T_{comp} = 112 ± 2K. One measurement was also made at 180K to provide a consistency check with the previous series of measurements [10]. This gave a total of seven measurements on the $Fe_{64}Er_{19}B_{17}$ glass at 1.5K, 60K, 100K 112K, 125K and 180K (× 2) and one measurement was also made on a $Fe_{78}Er_5B_{17}$ glass at 2K and 2T. This sample was more ductile and could be wound on a flat frame with appropriate cadmium shields. The data in all these scans were recorded with incident wavevectors $k_i = 2.662 Å^{-1}$ and $k_i = 4.1 Å^{-1}$. Some of the data points in the regions $Q \approx 3.1 Å^{-1}$, $4.3 Å^{-1}$ and $5.1 Å^{-1}$ can be contaminated by Bragg peaks from the cryomagnet or the sample holder. Since these Bragg peaks are intense in comparison with the small cross-sections, it was simplest to omit the contaminated points from the data. The analysis required to obtain the four spin-dependent scattering cross-sections in absolute units from the raw data, has been explained by us previously [1, 4, 12].

2.0) Magnetisation measurements *M(T) v. T* for the $Fe_{64}Er_{19}B_{17}$ glass

Figure 1 shows the four magnetisation curves *M(T) v. T* obtained for the $Fe_{64}Er_{19}B_{17}$ glass plotted in units of Am^2kg^{-1} and K. The data is almost identical to that obtained by Szymański *et al* on a $Fe_{66}Er_{19}B_{15}$ glass which is shown in Figure 1 of [9], including the field dependence of the magnetisation. The values of *M(T)* are low < $25Am^2kg^{-1}$ with minimum values at $T \approx$ 114K, where the ferrimagnetic compensation occurs. The true reversal of total magnetisation is not revealed because the absolute magnitude of the sublattice magnetisations $|M_{Fe}(T)+M_{Er}(T)|$ is measured [13].

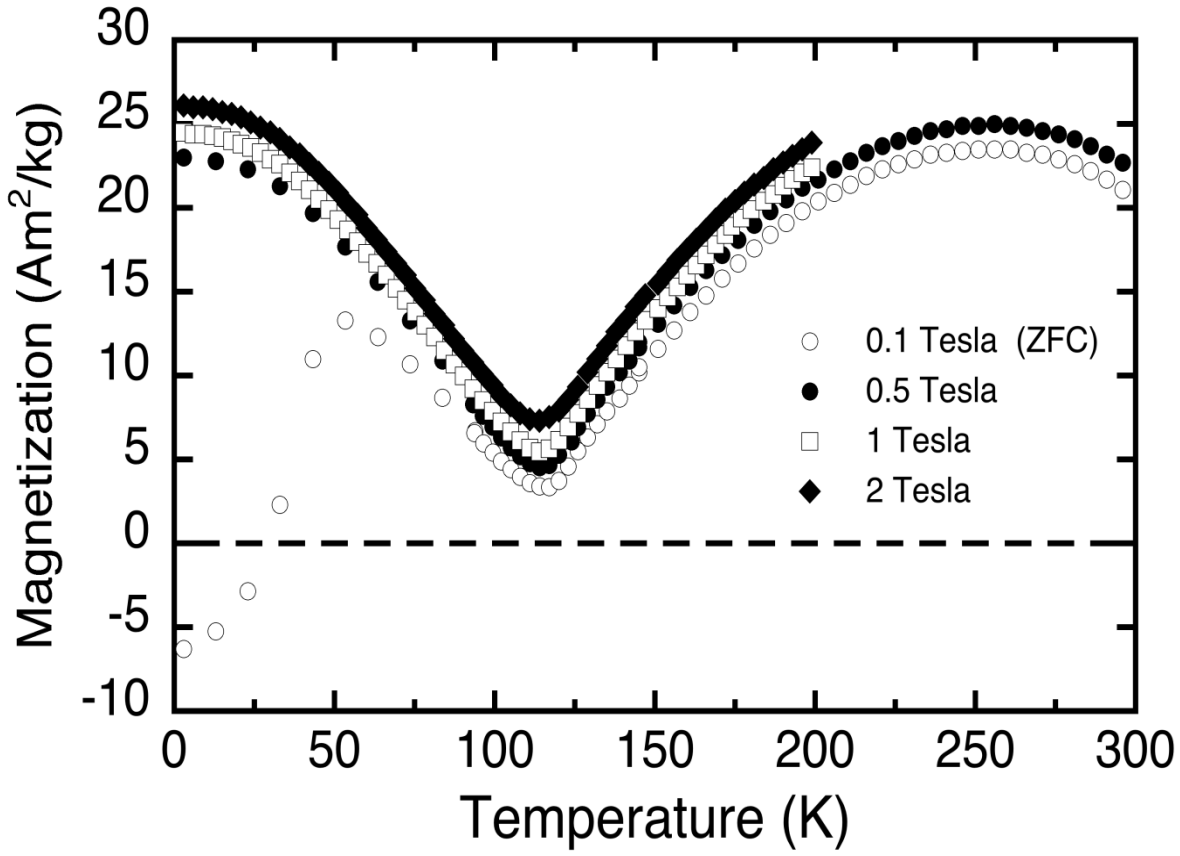

Figure 1 The bulk magnetisation *M(T) v. T* of the $Fe_{64}Er_{19}B_{17}$ glass is shown, measured in fields of 0.1T (zero field cooled), 0.5T, 1.0T and 2.0T. The minimum values of *M(T)* are at T ≈ 114K, close to the ferrimagnetic compensation temperature T_{comp} = 112 ± 2K, where the magnetisation direction actually reverses.

2.1) The sublattice magnetisations

The derivation of the spontaneous magnetisation curves $M(T)/M(0)\,v.\,T/T_{fN}$ and examples of the vector sum of the non-equivalent sublattices which describe the ferrimagnetism in the $(Fe,RE)_{83}B_{17}$ glasses are presented in all the standard textbooks [*e.g.* 13]. The data set at 0.5T from Figure 1, was taken as representative (and also measured over the wider temperature range) and converted to magnetic moment per atom, which is more convenient for the neutron experiments. The saturation value of $M(T) \approx 25\mathrm{Am^2kg^{-1}}$ corresponds to $\overline{\mu}^{\parallel} \approx 0.31\mu_B$ per atom which is similar to the moment of an Er^{3+} ion ($\mu_{Er} = 9.5\mu_B$) aligned antiparallel to the moment of an elemental iron atom ($\mu_{Fe} = -2.2\mu_B$) at the $Fe_{64}Er_{19}B_{17}$ concentration,

$$(0.19\times 9.5) - (0.64\times 2.2) = 0.40\,\mu_B.$$

The ferrimagnetic Néel temperature T_{fN} of the $Fe_{64}Er_{19}B_{17}$ glass is required to create the reduced magnetsisation curves $M(T)/M(0)\,v.\,T/T_{fN}$ but was outside the range of the measurements. The value $T_{fN} = 350$K was chosen after some trials and extrapolations and is similar to $T_{fN} = 330$K measured for a $Fe_{66}Er_{19}B_{15}$ glass [9].

Figure 2a shows a first attempt to describe the measured temperature variation of the mean collinear magnetic moment per atom $\overline{\mu}^{\parallel}_{meas}$, which has been plotted with a change of sign at T_{comp}. The two compositionally weighted contributions to $\overline{\mu}^{\parallel}_{calc}$ from the erbium and iron magnetic sub-lattices are represented by,

$$\overline{\mu}^{\parallel}_{Er} = 0.19 \times 9.5\mu_B \times M_{Er}(T)/M(0) \quad \text{obtained with } J = {}^{15}/_{2} \text{ and,}$$

$$\overline{\mu}^{\parallel}_{Fe} = -\,0.64 \times 2.2\mu_B \times M_{Fe}(T)/M(0) \quad \text{obtained with } J = S = ½.$$

The calculated variation of the mean collinear moment with temperature,

$$\overline{\mu}^{\parallel}_{calc} = \overline{\mu}^{\parallel}_{Er} - \overline{\mu}^{\parallel}_{Fe}$$

is shown by the dashed line which remains positive for all temperatures and obviously fails to imitate the experimental data.

The calculation was then reversed and the open points in Figure 2b show the variation of moment on the erbium atoms which would be *required* to produce the measured mean collinear moment $\overline{\mu}^{\parallel}_{meas}$,

$$\overline{\mu}^{\parallel}_{Er\ requ} = \overline{\mu}^{\parallel}_{meas} - \overline{\mu}^{\parallel}_{Fe}.$$

In order to produce the classic type of compensation in a ferrimagnet, the magnetisation of one sublattice has to fall more rapidly with temperature than the other [13]. Comparing $\overline{\mu}^{\parallel}_{Er}$ in Figure 2a with $\overline{\mu}^{\parallel}_{Er\ requ}$ in Figure 2b and ignoring the discontinuity, suggests that an

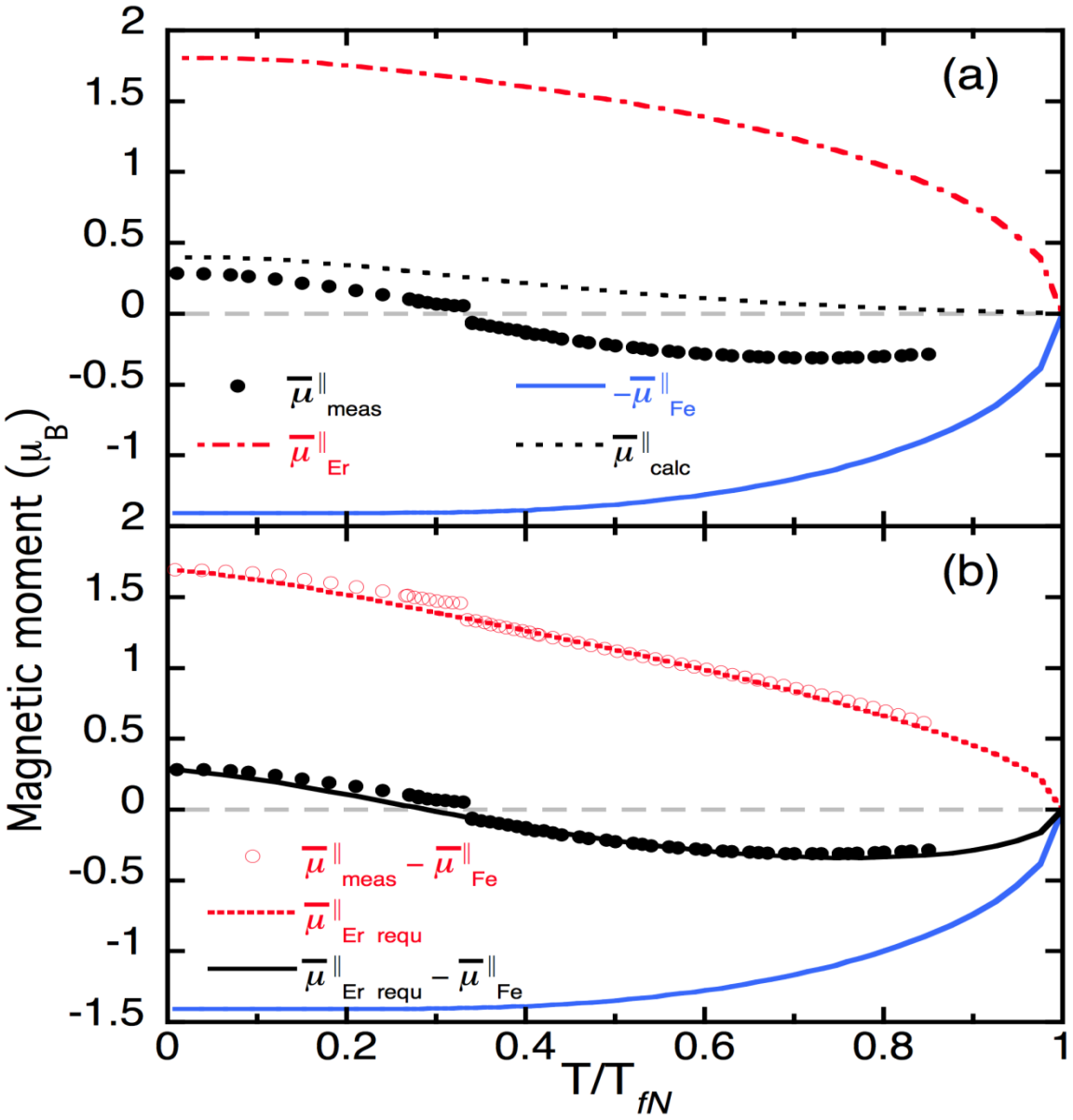

Figure 2 The measured temperature variation of the mean collinear magnetic moment per atom $\overline{\mu}^{\parallel}_{meas}$ in $Fe_{64}Er_{19}B_{17}$ glass is described by a model using the classical reduced magnetisation curves in Figure 2a and with a modified magnetisation curve for the erbium moments in Figure 2b.

arbitrary linear reduction to $\overline{\mu}^{\parallel}_{Er}$ would imitate the $\overline{\mu}^{\parallel}_{Er\ requ}$ successfully. Using the end points of the experimental data (0.008, 1.694) (0.845, 0.617) and the corresponding values of $\overline{\mu}^{\parallel}_{Er\ requ}$ gave a reduction factor of,

$$R\left(T/T_{fN}\right)=0.937-\left(0.384\times T/T_{fN}\right) \quad (1)$$

The new, smooth variation of the erbium moment with temperature $\overline{\mu}^{\parallel}_{Er\ requ}$ is shown by the dashed line in Figure 2b. The new variation of $\left(\overline{\mu}^{\parallel}_{Er\ requ}-\overline{\mu}^{\parallel}_{Fe}\right)$ with temperature is shown by the central continuous line in Figure 2b, which matches the corresponding data points very well. This figure is almost identical to the schematic figures which illustrate ferromagnetic compensation in the standard texts [13]. The ferrimagnetic compensation is predicted to occur at T/T_{fN} = 0.288, rather than at the minimum of *M(T)* at T/T_{fN} = 0.326.

Note that it has not been necessary to change the S = ½ curve for the iron sublattice in this demonstration. Intra-sublattice interactions generally cause the magnetisation of one sublattice to reduce more quickly than the other and here they may be attributed to variations in the random cone angle of the erbium sublattice. In a "filled cone" structure, the magnitude of the magnetic moments remains unchanged and they point at all angles to the magnetic field within the cone . The mean component of the collinear moments is then given by [9],

$$\overline{\mu}^{\parallel}=\mu\left(1+\cos\theta\right)/2 \quad (2)$$

where θ is the semi-vertex angle of the cone. Alternatively the reduction could be caused by a minority of the erbium moments orientated antiparallel to the majority, which has been proposed for the iron sublattice in [9].

2.2) Refinement of the model

Figure 2 shows that it is feasible to describe the magnetisation curves of the $Fe_{64}Er_{19}B_{17}$ glass using a model in which the erbium and iron atoms carry similar moments to those in their elemental state. To refine this model, the actual moment values $\left|\mu_{Fe}\right|$ and $\left|\mu_{Er}\right|$ at the $Fe_{64}Er_{19}B_{17}$ composition are required. We have previously used a Linear Reducing Model (LRM) to describe the variation of magnetic moment in the $(Fe,RE)_{83}B_{17}$ glasses [4, 12], where the iron and rare earth moments have their elemental values at small rare earth concentrations and fall linearly with composition to the point where the ferrimagnetism is suppressed [4, 14]. This concentration is higher in the $(Fe,Er)_{83}B_{17}$ glasses, because the moments are better sustained [5, 6] and an LRM with Er ≈ 80% gives the saturation values of the total moments, μ_{Fe} = 1.68μ_B and μ_{Er} = 7.24μ_B for $Fe_{64}Er_{19}B_{17}$ [12]. At low temperatures, random cone angles of $\theta_{Fe} \approx 36^o$ and $\theta_{Er} \approx 60^o$ have been suggested [9], so Equation 2 gives $\overline{\mu}^{\parallel}_{Fe}$ = 1.52μ_B and $\overline{\mu}^{\parallel}_{Er}$ = 4.53μ_B for the parallel components at saturation.

The steps shown in Figure 2a were applied again to the data, using these new moment values. The compositionally weighted contribution to $\overline{\mu}^{\parallel}$ from the iron $\overline{\mu}^{\parallel}_{Fe\ adj}$ magnetic sub-lattice is,

$$\overline{\mu}^{\parallel}_{Fe\ adj} = \pm\ 0.64 \times 1.52\mu_B \times M_{Fe}(T)/M(0) \quad \text{obtained with } J = S = ½, \tag{3}$$

which describes a reduction in moment caused by a non-collinear state which follows a conventional magnetisation curve. This simplification can probably be defended because the random cone angles in the iron sublattice are relatively small. The subscript *adj* in Equation 3 means the moment values have been adjusted to the $Fe_{64}Er_{19}B_{17}$ composition and the positive and negative signs correspond to the temperatures above and below T_{comp} respectively. The graph of Equation 3 and the experimental data were used as before, to deduce the adjusted variation of the contribution from the erbium moments needed to produce the measured data,

$$\mu^{\parallel}_{Er\,adj} = \mp\ 0.64 \times \overline{\mu}^{\parallel}_{Er} \times M_{Er\ adj}(T)/M(0) \tag{4}$$

The calculations showed that the LRM had underestimated the value of $\overline{\mu}^{\parallel}_{Er}$ which had to be increased to $\overline{\mu}^{\parallel}_{Er} = 6.61\mu_B$, although its variation with temperature was still adequately described by a linear correction,

$$R(T/T_{fN}) = 1.462 - (0.796 \times T/T_{fN}). \tag{5}$$

The intercept and slope of the correction terms are different in Equations 1 and 5, since the proportionality between the $\overline{\mu}^{\parallel}_{Fe}$ and $\overline{\mu}^{\parallel}_{Er}$ moments has now changed because of the different values of θ_{Fe} and θ_{Er} given above.

These parameters can be changed *slightly* to ensure that the minimum of the calculated curve is close to the minimum in the experimental data which has the co-ordinates (0.331, 0.057). Changing either of the values of $\overline{\mu}^{\parallel}_{Fe}$ or $\overline{\mu}^{\parallel}_{Er}$ gives better agreement one side of T_{comp} and worse agreement on the other. Allowing the value of $\overline{\mu}^{\parallel}_{Er}$ to fall less rapidly with temperature (by altering the slope in Equation 5) moves the calculated value of T_{comp} to higher temperatures. The calculated curve is very sensitive to this and a 7% reduction of the slope to 0.746 was sufficient to produced the best agreement. The value of T/T_{fN} at which the structural reversal occurs was also adjusted slightly, but this always produced discontinuities in the calculated curve. The best overall agreement between the calculated curve and the experimental data is shown in Figure 3a, which is plotted to illustrate the reversal of the two magnetic sublattices at T_{comp} and with the experimental data presented in the same way as in Figure 1. The level of agreement is quite satisfactory given the relative

simplicity of the model. The mean values of the collinear components of the moments $\left|\mu^{\parallel}_{Fe\ adj}\right|$ and $\left|\mu^{\parallel}_{Er\ adj}\right|$ are presented in Figure 3b, together with their weighted mean. Whilst.

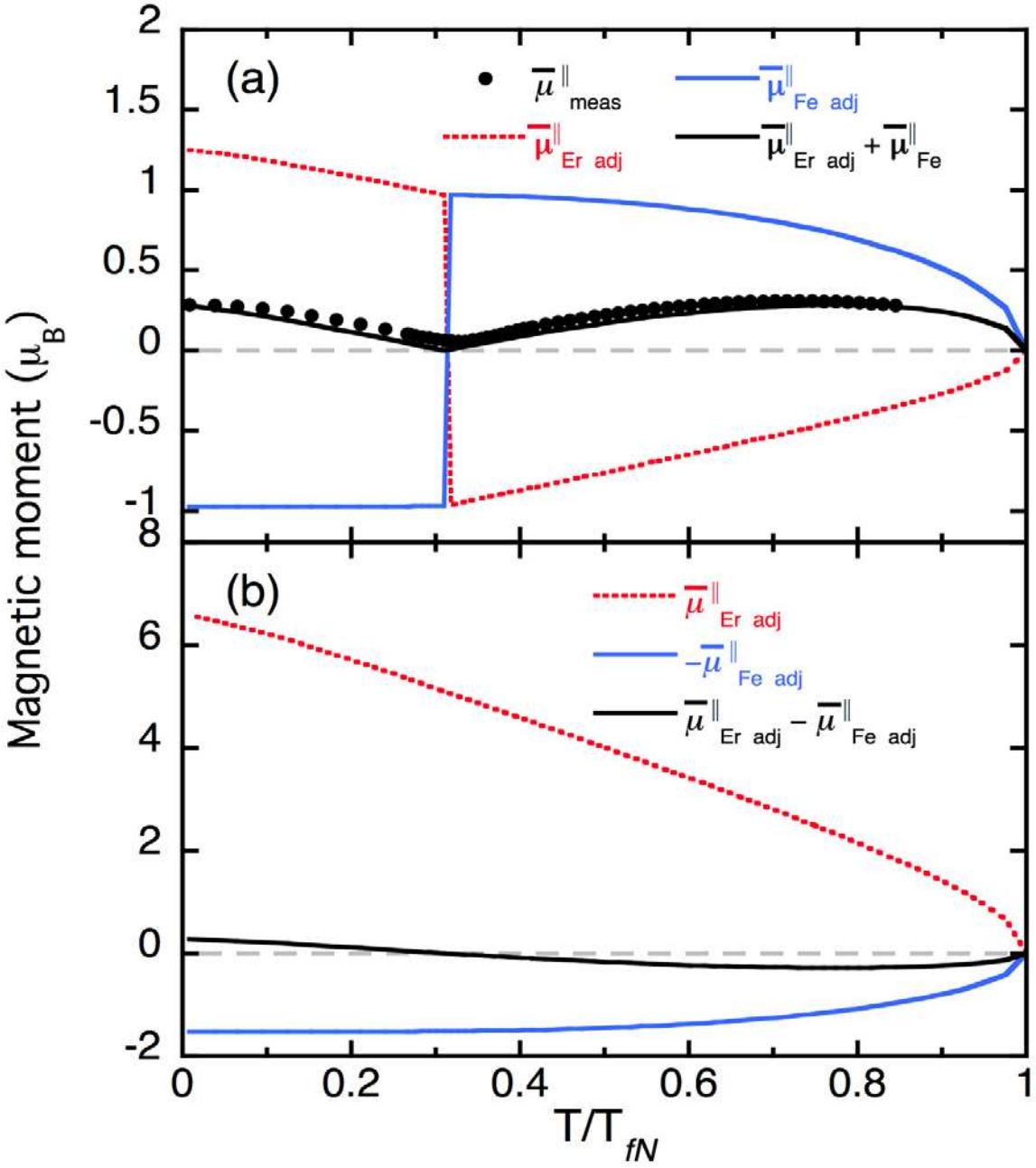

Figure 3 The measured variation of the mean collinear magnetic moment per atom $\overline{\mu}^{\parallel}$ in $Fe_{64}Er_{19}B_{17}$ glass is compared with a calculated variation based on $\left(\overline{\mu}^{\parallel}_{Er\ adj} + \overline{\mu}^{\parallel}_{Fe\ adj}\right)$ in Figure 3a. The reversal of the two magnetic sublattices at T_{comp} is depicted and the experimental data is presented in the same style as in Figure 1. The values of $\mu^{\parallel}_{Er\,adj}$ and $\mu^{\parallel}_{Fe\ adj}$ in Figure 3b show how they combine to give small values of $\overline{\mu}^{\parallel}$ over the whole temperature range.

the two moment values are quite different, they produce a small net moment over most of the temperature range

2.3) Magnetic moment values and the transition at T_{comp}

The mean parallel components of the moments $\overline{\mu}_{Er}^{\parallel}$ and $\overline{\mu}_{Fe}^{\parallel}$ from the magnetisation data are given in the middle columns of Table 1. The values which were used previously in the calculation of three spin-flip cross-sections [12] are given in the left hand columns of the Table. They were based on an LRM and on the published literature [5, 6, 9]. The Table shows that the values of $\overline{\mu}_{Fe}^{\parallel}$ at 1.5K and 60K (which are both close to saturation conditions) and of $\overline{\mu}_{Er}^{\parallel}$ at 180K ($3.64\mu_B$: $3.92\mu_B$) and 60K ($5.15\mu_B$: $5.82\mu_B$) are comparable in both studies. However, the new value of $\overline{\mu}_{Fe}^{\parallel}$ at 180K ($1.45\mu_B$) is larger by ≈ 17% and that of $\overline{\mu}_{Er}^{\parallel}$ at 1.5K ($4.56\mu_B$: $6.58\mu_B$) appears to have been underestimated in [12]. An underestimate of the size of the moment can of course, be compensated in the calculations of the spin-flip cross-sections, by just increasing the cone angle θ_{Er}. The moment values at 112K in Table 1 are obviously consistent with the ferromagnetic compensation

$$0.64\,\overline{\mu}_{Fe}^{\parallel} - 0.19\,\overline{\mu}_{Er}^{\parallel} = 0.64\times1.51 - 0.19\times5.06 \approx 0.005\mu B.$$

Comparing the present moment values with those obtained elsewhere, the new value of $\overline{\mu}_{Er}^{\parallel}$ = $6.58\mu_B$ means that the total moment on the erbium atoms must be in the region of $\mu_{Er} \approx 8.8\mu_B$, if the random cone angle is $\theta_{Er} \approx 60°$ as suggested in [9]. Our previous experience with the $(Fe,Tb)_{83}B_{17}$ glasses [4, 14] led us to doubt that the erbium moment in the $(Fe,Er)_{83}B_{17}$ glasses changed slowly on alloying [6, 7], but this indeed appears to be the case. Information from previous magnetisation and Mössbauer spectroscopy measurements [5, 6, 9] on similar samples has already been incorporated into the present analysis, so this has led a measure of agreement. The moment values obtained from XMCD measurements on Fe,Er amorphous thin films [7, 8] on the other hand, appear to be consistently higher than the present values, even allowing for the fact that the moment values in binary Fe,Er amorphous alloys [6] are always ≈ $0.5\mu_B$ greater than in ternary (Fe,Er)-met glasses [6, 5]. In addition to this discrepancy, preliminary results from recent XCMD measurements on material from our own $Fe_{64}Er_{19}B_{17}$ sample, suggest that the reversal of the magnetic structure at T_{comp} may not be sharp, but take place over a large temperature range ≈ 100K [15]. The calculations of the magnetisation curves were therefore modified to imitate a gradual reversal of the magnetic structure, by using temperature-dependent weighting factors for the two sublattices over the

range $T < 25\text{K} < T < 150\text{K}$. The resulting curve was more rounded; in poorer agreement with the data and failed to give the depth at the minimum in $\overline{\mu}^{\parallel}_{meas}$ at T_{comp}.

To summarise, the analysis of the magnetisation data has given a set of $\overline{\mu}^{\parallel}_{Fe}$ and $\overline{\mu}^{\parallel}_{Er}$ moment values for the $Fe_{64}Er_{19}B_{17}$ glass at the same temperatures 1.5K, 60K, 100K 112K, 125K, 180K as the neutron measurements. It will be shown in the next Section that they lead, with minimal refinement, to a coherent analysis of the spin-flip neutron scattering cross-sections and thus provide a description of the non-collinear structures in this glass and their variation with temperature.

Sample and temperature	T/T_{fN}	Mean collinear components $\overline{\mu}^{\parallel}$ of the magnetic moment in μ_B					
		from an LRM [12]		from $M(T)$ *v.* T		from the calculations of $\frac{\partial\sigma^{\pm\mp}}{\partial\Omega}$	
		$\overline{\mu}^{\parallel}_{Fe}$	$\overline{\mu}^{\parallel}_{Er}$	$\overline{\mu}^{\parallel}_{Fe}$	$\overline{\mu}^{\parallel}_{Er}$	$\overline{\mu}^{\parallel}_{Fe}$	$\overline{\mu}^{\parallel}_{Er}$
$Fe_{0.78}Er_{0.05}B_{0.17}$							
2K	-	-	-	-	-	1.87	8.00
$Fe_{0.64}Er_{0.19}B_{0.17}$							
180K	0.517	1.23	- 3.64	1.45	- 3.92	1.46	- 3.83
180K	0.517	-	-	1.45	- 3.92	1.46	- 3.84
125K	0.353	-	-	1.51	- 4.89	1.50	- 4.66
112K	0.318	-	-	1.51	- 5.06	1.13	- 3.79
112K (2)	0.318	-	-	1.51	5.06	0.00	0.00
100K	0.284	-	-	- 1.52	5.25	- 1.51	5.25
60K	0.182	- 1.53	5.15	- 1.52	5.82	- 1.52	5.81
1.5K	0.008	- 1.52	4.56	- 1.52	6.58	- 1.52	6.56

Table 1 The mean collinear components $\overline{\mu}^{\parallel}_{Fe}$, $\overline{\mu}^{\parallel}_{Er}$, of the magnetic moments are given in μ_B. The left hand columns give the values derived from a linear reducing model (LRM) in [12]; the middle columns give the values from the magnetisation measurements and the right hand columns give the refined values from the calculations of the spin flip cross-sections, which will be presented in Section 3.

3.0) Analysis of the spin-flip cross-sections of the $(Fe,Er)_{83}B_{17}$ glasses.

The two non spin-flip cross-sections and the two spin-flip cross-sections are measured sequentially at each data point in the polarised beam neutron scattering experiments. The spin-flip cross-sections obtained with the present experimental configuration are defined in Equation 6 using the normal notation, where $\frac{\partial\sigma_{NSI}}{\partial\Omega}$ is the nuclear spin incoherent cross-section and the superscripts (+/-) refer to the initial and final spin states of the neutron,

$$\frac{\partial\sigma^{\pm}}{\partial\Omega} = \frac{\partial\sigma^{\mp}}{\partial\Omega} = \frac{2}{3}\frac{\partial\sigma_{NSI}}{\partial\Omega} + \left|\left\langle\sum_{ij}\frac{1}{2}\left(p_i^{\perp}(Q)\,p_j^{\perp *}(Q)\right)\exp\left(iQ.\left(r_i - r_j\right)\right)\right\rangle\right|. \qquad (6)$$

They depend on the ***non-collinear components*** $p^{\perp}(Q)$ of the magnetic scattering amplitude,

$$p^{\perp}(Q) = 2.695\,\mu^{\perp} f(Q) \text{ fm.} \qquad (7)$$

which contains the non-collinear component of the magnetic moment $\mu^{\perp}$ in Bohr magnetons and *f(Q)* the magnetic form factor, which lies between 0 and 1 [16]. When the spin-flip cross-sections are larger than $\frac{2}{3}$ of the nuclear spin incoherent cross section $\frac{\partial\sigma_{NSI}}{\partial\Omega}$, they provide direct evidence of a non-collinear configuration of the magnetic moments which has finite $\mu^{\perp}$ values.

Figure 4 shows the mean of the two $\frac{\partial\sigma^{\pm}}{\partial\Omega}$, $\frac{\partial\sigma^{\mp}}{\partial\Omega}$ spin-flip cross-sections in absolute units of barns steradian^{-1} atom^{-1} for the $Fe_{78}Er_5B_{17}$ glass measured at 2K and for the $Fe_{64}Er_{19}B_{17}$ glass measured at 1.5K, and 60K (from [12]) and the present measurements at 100K, 112K, 125K and 180K. All of these spin-flip cross-sections are finite with a negative slope and they are all greater than the nuclear spin incoherent cross-section. This shows that there are non-collinear magnetic structures in both glasses, which exist over an extended temperature range in $Fe_{64}Er_{19}B_{17}$.

If the magnetic moments point in random directions with no spatial correlations, the second term in Equation 6 reduces to $\left\langle p^{\perp\,2}(Q)\right\rangle$ and the cross-sections follow a form-factor dependence with *Q*,

$$\frac{\partial\sigma^{\pm}}{\partial\Omega} = \frac{\partial\sigma^{\mp}}{\partial\Omega} = 0.0362\left[c_{Fe}\,\overline{\mu}_{Fe}^{\perp\,2}\,f_{Fe}^2(Q) + c_{Er}\,\overline{\mu}_{Er}^{\perp\,2}\,f_{Er}^2(Q)\right] \qquad (8)$$

in units of barns steradian^{-1} atom^{-1}. This behaviour is illustrated in Figure 4.

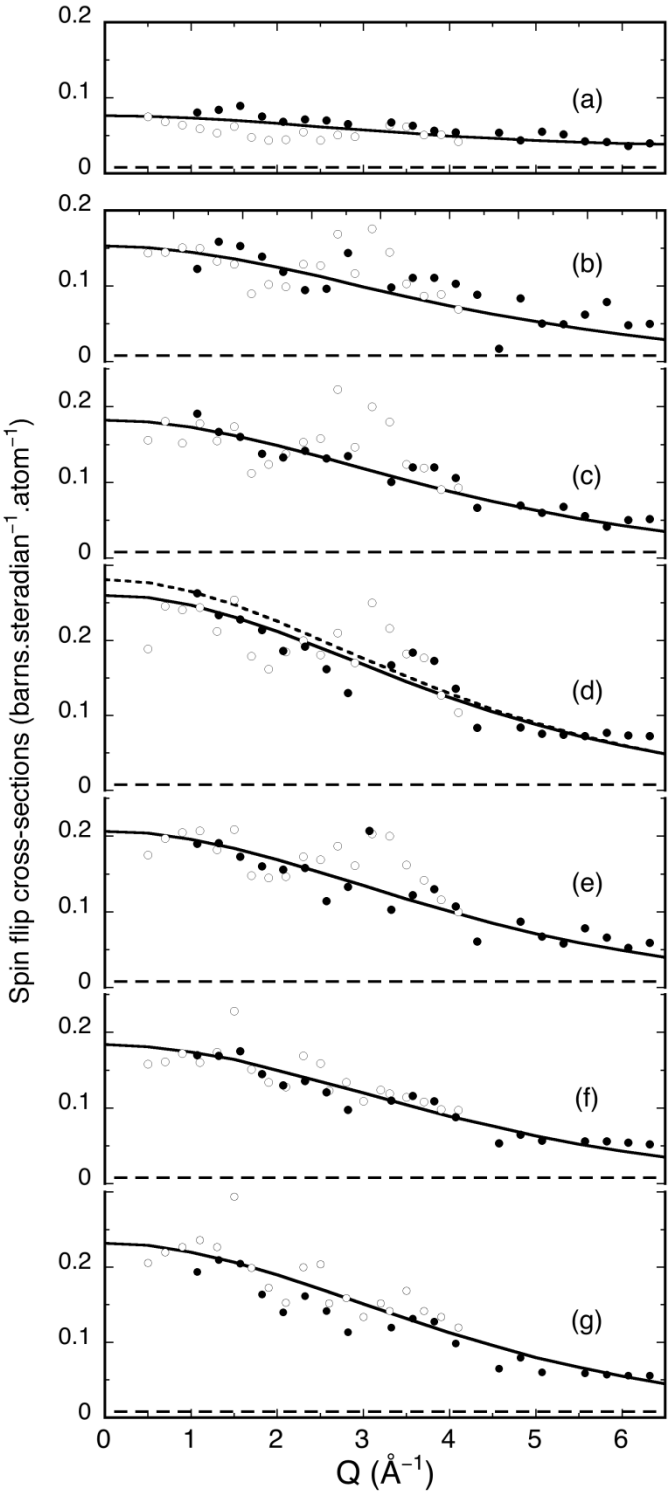

Figure 4 The mean of the two spin-flip cross-sections $\partial\sigma^{\pm}/\partial\Omega, \partial\sigma^{\mp}/\partial\Omega$ for the $Fe_{78}Er_5B_{17}$ glass at 2K are shown in 4a and for the $Fe_{64}Er_{19}B_{17}$ glass at 180K 4b, 125K 4c, T_{comp} = 112K 4d, 100K 4e, 60K 4f[12] and 1.5K 4g[12]. The open points ○ are with $k_i = 2.662$Å^{-1} and the closed points ● with $k_i = 4.1$Å^{-1}. The incoherent cross-section is shown by the dashed line and the solid and dotted lines are the calculated cross-sections.

Calculations were made of these spin-flip cross-sections, - since it is not really practical to *fit* the experimental data, because of the myriad choices of the input parameters in the calculations and the rather limited Q range of the data. Starting with the $Fe_{64}Er_{19}B_{17}$ glass, the total moments $|\mu_{Fe}|$ and $|\mu_{Er}|$ were based on the LRM described in Section 2 and their components $\overline{\mu}_{Fe}^{\parallel}$, $\overline{\mu}_{Er}^{\parallel}$ and $\overline{\mu}_{Fe}^{\perp}$, $\overline{\mu}_{Er}^{\perp}$, were calculated for "filled-cone" structures with semi-vertex angles $0 < \theta < 90°$. The components of the collinear moments are [9],

$$\overline{\mu}^{\parallel} = \mu(1+\cos\theta)/2 \qquad \text{(previously Eq 2)}$$

and

$$\overline{\mu}^{\parallel 2} = \mu^2(1+\cos\theta+\cos^2\theta)/3 \qquad (9)$$

The values of the corresponding $\overline{\mu}_{Fe}^{\perp 2}, \overline{\mu}_{Er}^{\perp 2}$ components were tabulated against θ and used with Equation 8 to identify the possible contributions to $\left|\frac{\partial\sigma}{\partial\Omega}^{\pm\mp}\right|_{Q=0}$ from the two magnetic sublattices. The Q-dependence of the cross-sections was introduced using the seven parameter fits to the form factors of the Fe^{3+} and Er^{3+} ions from [16]. The relative contributions from the erbium and iron sublattices to Equation 8 are significant, because their form factors have different Q dependence and change the shape of the calculated cross-section. The curves calculated over $0 < Q < 7.0$ Å^{-1} were finally superimposed on the experimental data and the process was repeated systematically for small changes of the input parameters, until it was judged that the best agreement between the calculation and the data had been obtained. The continuous lines in Figure 4 show the calculated spin-flip cross-sections.

The important new input to these calculations in comparison with [12], was that whilst the $\overline{\mu}_{Fe}^{\perp 2}$ and $\overline{\mu}_{Er}^{\perp 2}$ components were being chosen to produce the calculated spin-flip cross-sections, they were also required to be consistent with the collinear components $\overline{\mu}_{Er}^{\parallel}$, $\overline{\mu}_{Fe}^{\parallel}$ which were obtained in Section 2. A comparison of the middle and the right hand columns of Table 1 shows that this was achieved in every case, except at T = 112K, where the $\overline{\mu}_{Er}^{\parallel}$, $\overline{\mu}_{Fe}^{\parallel}$ values which emerged from calculating the spin-flip cross-sections were smaller than those obtained from the magnetisation data.

Table 2 gives the moment components $\overline{\mu}^{\perp 2}$, $\overline{\mu}_{Fe}^{\perp 2}$, $\overline{\mu}_{Er}^{\perp 2}$ and the random cone angles θ_{Fe}, θ_{Er} which were used to calculate the spin-flip cross-sections at each temperature. The two

data sets at 180K, which were obtained in two quite different experimental periods on IN20, yielded almost identical parameters given in adjacent rows of the Table. This confirms the internal consistency of these experiments and their analysis. Figure 4 shows that the spin-flip cross-section at 112K is the largest one measured and in the row labelled 112K the cone angles θ_{Fe}, θ_{Er} have been increased to account for this. The $\overline{\mu}_{Er}^{\parallel}$, $\overline{\mu}_{Fe}^{\parallel}$ are then reduced, as observed, since the total moments $|\mu_{Fe}|$ and $|\mu_{Er}|$ do not change significantly over the temperature range 100K – 112K – 125K. The parameters in the row 112K (2) data will be described in Section 3.2 below.

			Magnetic moment μ_{Fe}			**Magnetic moment μ_{Er}**		
Sample and temperature	$\frac{\partial\sigma^{\pm\mp}}{\partial\Omega}_{Q=0}$ in bst^{-1} at^{-1}	$\overline{\mu}^{\perp 2}$ in μ_B^2	$\|\mu_{Fe}\|$ in μ_B	θ_{Fe}°	$\overline{\mu}_{Fe}^{\perp 2}$ in μ_B^2	$\|\mu_{Er}\|$ in μ_B	θ_{Er}°	$\overline{\mu}_{Er}^{\perp 2}$ in μ_B^2
$Fe_{0.78}Er_{0.05}B_{0.17}$								
2K	0.045	1.24	2.00	30º	0.51	9.00	39º	16.71
$Fe_{0.64}Er_{0.19}B_{0.17}$								
180K	0.146	4.02	1.60	34º	0.41	6.00	74º	19.78
180K	0.153	4.21	1.60	34º	0.41	6.10	75º	20.77
125K	0.182	5.01	1.645	35º	0.46	6.95	70º	24.81
112K	0.264	7.23	1.65	68.5º	1.36	7.20	87º	33.61
112K (2)	0.281	7.74	1.65	180º	1.82	7.20	180º	34.56
100K	0.206	5.68	1.66	35º	0.47	7.60	62.5º	28.32
60K	0.184	5.06	1.67	35º	0.47	7.75	60º	25.03
1.5K	0.232	6.38	1.68	36º	0.50	8.75	60º	31.90

Table 2 The forward limit $\left|\partial\sigma^{\pm\mp}/\partial\Omega\right|_{Q=0}$ of the spin-flip cross-sections and the mean square values of the non-collinear moments $\overline{\mu}^{\perp 2}$ are given as a function of temperature. The parameters used to calculate the spin-flip cross-sections; the total moments $|\mu|$; their mean square non-collinear components $\overline{\mu}^{\perp 2}$ and the random cone angles θ are also given.

The calculation of the mean spin-flip cross-section of the $Fe_{78}Er_5B_{17}$ glass measured at 2K and 2T was more difficult for a number of reasons. First, it was the smallest cross-section in

magnitude and subject to the largest statistical uncertainty. The magnetic moment values were less well known and there were also some *small* systematic differences between the data recorded with the $k_i = 2.662$Å^{-1} and $k_i = 4.1$Å^{-1} incident beams. Such small cross-sections are difficult to measure with complete confidence, because they are close to the experimental limits. Their absolute magnitude is also influenced by *small* variations in the polarisation corrections which have virtually no effect on the magnitudes of the larger non spin-flip cross-sections.

Rather than trying to obtain meaningful parameters from this mean cross-section, the calculations were used to show that it was consistent with the non-collinear structure which was proposed in [5] and even then a small adjustment had to be made to its absolute magnitude. The "empty cone" structure with $|\mu_{Er}| = 9.0\mu_B$ and $\theta_{Er} = \cos^{-1}(8/9) = 27°$ [5] was imitated with a "filled cone" structure (to use the same computer codes) with a larger cone angle to give the same value of $\overline{\mu}^{\perp 2}$. The parameters of the calculation are given in Table 2 and the continuous line on the data in Figure 4 suggests that the cross-section is at least consistent with the presence of a non-collinear structure in $Fe_{78}Er_5B_{17}$ at 1.5K.

3.1) Random cone or spatially correlated magnetic structures in $Fe_{64}Er_{19}B_{17}$ glass?

The measured spin-flip cross sections of $Fe_{78}Er_5B_{17}$ and of $Fe_{64}Er_{19}B_{17}$ at 1.5K. 60K and 180K follow a form factor dependence with Q quite well, although the data points of the cross-sections for $Fe_{64}Er_{19}B_{17}$ at 100K. 112K and 125K suggest that there might also be a sharper feature around $Q \approx 3.1$Å^{-1}. The form factor dependence with Q corresponds to a random (uncorrelated) arrangement of magnetic moments and departures from this imply the presence of *spatial correlations between the non-collinear components* $\mu_{Fe}^{\perp}$ and $\overline{\mu}_{Er}^{\perp}$. A strong positive feature in a scattering cross-section at Q_p leads, in a sine Fourier transform, to a positive feature in real space at $r_p = \frac{5}{4}\frac{2\pi}{Q_p}$, - see pages 847-9 of [17]. Using this relation with $Q \approx 3.1$Å^{-1}, gives a radial distance of $r \approx 2.6$Å which is similar to the weighted mean first neighbour distance (2.63Å) in $Fe_{64}Er_{19}B_{17}$ obtained using the Goldschmidt radii of the metal atoms and the tetrahedral covalent radius of boron. If such a feature existed in the spin-flip cross-sections, it would mean that there were correlations between the $\overline{\mu}_{Fe}^{\perp}$, $\overline{\mu}_{Er}^{\perp}$ components at the first neighbour distance, - at least for those temperatures close to T_{comp}. Unfortunately, the statistical quality of the data and the spacing of the data points do not

permit a clear feature to be defined. Each of these neutron measurements took several hours, so that scans of one or more days would be needed to improve their statistical quality significantly. This would be difficult to arrange given the heavy overload on the IN20 instrument. In any case, the Fourier transform of a *single* peak at a fixed value of Q provides little information in real space, other than the characteristic distance r and possibly a basic periodicity, as explained in the context of metallic glasses in Figure 12 of [18].

3.2) Evidence for a compensated sperimagnetic phase in the $Fe_{64}Er_{19}B_{17}$ glass at T_{comp}.

Equation 8 shows that when $Q = 0$ and $f_{Fe}(Q)$ and $f_{Er}(Q)$ are both unity, the term in the square brackets is the compositional average of the square of the non-collinear moments $\overline{\mu}^{\perp 2}$.The forward limit $\left|\partial\sigma^{\pm\mp}/\partial\Omega\right|_{Q=0}$ of the spin-flip cross-sections and the values of $\overline{\mu}^{\perp 2}$, of the $Fe_{64}Er_{19}B_{17}$ glass are given in Table 2 and the values of $\left|\partial\sigma^{\pm\mp}/\partial\Omega\right|_{Q=0}$ are plotted as a function of temperature in Figure 5. At 112K, $\left|\partial\sigma^{\pm\mp}/\partial\Omega\right|_{Q=0}$ = 0.262 barns steradian^{-1} atom^{-1} is 26% and 46% greater than the two neighbouring values at 100K and 125K respectively. The total moments $|\mu_{Fe}|$ $|\mu_{Er}|$ are fixed at a given temperature and the mean square non-collinear components $\overline{\mu}_{Fe}^{\perp 2}, \overline{\mu}_{Er}^{\perp 2}$ have their maximum values when the random cone angles θ_{Fe} , θ_{Er} tend to 180°. It was explained in Section 3.0, that the random cone angles θ_{Fe} , θ_{Er} had to be increased in calculating the spin-flip cross-sections at 112K, which led to smaller values of the $\overline{\mu}_{Er}^{\parallel}$, $\overline{\mu}_{Fe}^{\parallel}$ components from those obtained from the magnetisation data. This suggests that it may be necessary to make a distinction between the ***general variation*** of the magnetisation with temperature and what happens at ***exactly*** T_{comp}. The calculation of the spin-flip cross-section at 112K was repeated using the values,

$$|\mu_{Fe}| = 1.65\mu_B, \ \theta_{\mathrm{Fe}} = 180^{\circ} \text{ and } |\mu_{Er}| = 7.2\mu_B, \ \theta_{\mathrm{Er}} = 180^{\circ}.$$

These parameters describe a special ***compensated sperimagnetic state***, since Equations 2 and 9 show that the mean components $\overline{\mu}_{Fe}^{\parallel}$, $\overline{\mu}_{Er}^{\parallel}$ go to zero when the cone angles θ_{Fe}, θ_{Er} go to 180° and the sample has no net magnetisation. This is somewhat similar to the speromagnetic state defined by Hurd as a sub-phase of ferromagnetism, in which "localised moments of a given species are locked into random orienatations with no net magnetisation" [10]. The main difference is that two different magnetic species are involved here rather than one. Note that

under the conditions given above the mean square components $\overline{\mu}_{Fe}^{\parallel\,2}$, $\overline{\mu}_{Er}^{\parallel\,2}$, $\overline{\mu}_{Fe}^{\perp\,2}$, $\overline{\mu}_{Er}^{\perp\,2}$, remain finite as ⅓ and ⅔ of their total value respectively and this is what maximises the spin-flip cross-sections. The calculated spin-flip cross section for this second configuration is shown by the dashed line in Figure 4 and the parameters for this calculation are given in the row marked 112K (2) in Tables 1 and 2. Since the second calculation (dashed line) gives a *slightly less good* match to the data than the first (solid line), the identification of the compensated sperimagnetic state at T_{comp} cannot be made with confidence from Figure 4 alone.

The sum and difference of the nuclear and collinear magnetic scattering amplitudes $\left(b \pm p^{\parallel}(Q)\right)$ will be required in the analysis of the non spin-flip cross-sections in **Part II** and they provide further evidence of this compensated sperimagnetic state at T_{comp}. They were calculated using the accepted values of the nuclear scattering amplitudes b [19] and the $p^{\parallel}(Q)\big|_{Q=0}$ obtained by substituting the $\overline{\mu}_{Fe}^{\parallel}$, $\overline{\mu}_{Er}^{\parallel}$ values from the right hand columns of Table 1

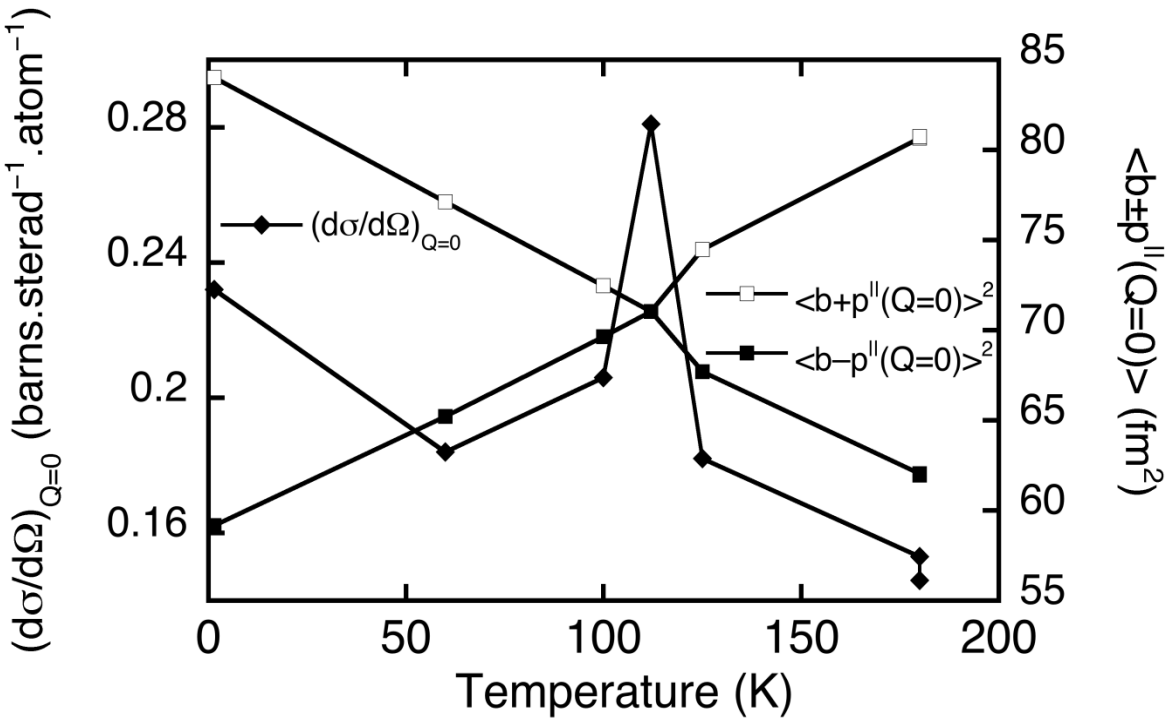

Figure 5 The forward limit $\left|\partial\sigma^{\pm\mp}/\partial\Omega\right|_{Q=0}$ of the spin-flip cross-sections of the $Fe_{64}Er_{19}B_{17}$ glass is plotted as a function of temperature and its value peaks around T_{comp} = 112K. The compositional averages of $\left\langle\left(b-p^{\parallel}(Q)\right)\right\rangle^2$ and $\left\langle\left(b+p^{\parallel}(Q)\right)\right\rangle^2$ are plotted and the two lines cross close to $T_{comp} \approx$ 112K.

into an equivalent of Equation 7. The compositional averages of $\left\langle \left| b + p^{\parallel}(Q) \right| \right\rangle^2 \Big|_{Q=0}$ and $\left\langle \left| b - p^{\parallel}(Q) \right| \right\rangle^2 \Big|_{Q=0}$ are plotted as a function of temperature in Figure 5. The data from row 112K (2) in Table 1 was used to plot this Figure, but even omitting that point the graphs of $\left\langle \left| b + p^{\parallel}(Q) \right| \right\rangle^2 \Big|_{Q=0}$ and $\left\langle \left| b - p^{\parallel}(Q) \right| \right\rangle^2 \Big|_{Q=0}$ will clearly cross close to T_{comp} = 112K. It is most unlikely that this could occur because of a numerical coincidence between the values of the *b*s and $p^{\parallel}(Q)$s (which would need to exist over five different temperatures). The obvious interpretation is that the $\overline{\mu}_{Fe}^{\parallel}$, $\overline{\mu}_{Er}^{\parallel}$ components go to zero at T_{comp} because a compensated sperimagnetic state is established at precisely the point of the ferrimagetic compensation. This will be discussed again in **Part II.**

4) Conclusions

Magnetisation measurements *M(T) v. T* on a $Fe_{64}Er_{19}B_{17}$ glass were analysed to identify the components of the magnetic moments needed to interpret the neutron scattering data on this glass. A phenomenological description of the magnetisation was used in which the magnetisation on the erbium sublattice fell more rapidly with temperature than the reduced magnetisation curve with $J = {}^{15}/_{2}$. This was refined using magnetic moment values appropriate to the $Fe_{64}Er_{19}B_{17}$ composition. Polarised beam neutron measurements were made on $Fe_{78}Er_5B_{17}$ and $Fe_{64}Er_{19}B_{17}$ glasses to supplement earlier measurements on $Fe_{64}Er_{19}B_{17}$. The finite spin-flip cross-sections confirmed that these $(Fe,Er)_{83}B_{17}$ glasses are non-collinear ferrimagnets, which can be described by a sperimagnetic structure in which the magnetic moments on the iron atoms point in a random cone that is antiparall to a random cone of erbium moments. The non-collinear components of the moments $\overline{\mu}_{Fe}^{\perp\,2}$ and $\overline{\mu}_{Er}^{\perp\,2}$ required to calculate the neutron spin-flip cross-sections were chosen to be compatible with the collinear components of the moments $\overline{\mu}_{Er}^{\parallel}$, $\overline{\mu}_{Fe}^{\parallel}$ from the magnetisation data, as well as the values of the random cone angles obtained elsewhere from bulk measurements [9]. The moment values from the magnetisation data needed little refinement to produce a consistent description of the measured spin-flip cross-sections. The temperature variation of the cross-sections and of the collinear components of the total scattering amplitudes $\left(b \mp p^{\parallel}(Q) \right)\Big|_{Q=0}$ suggested the presence of a special compensated sperimagnetic phase at T_{comp} = 112K. The

ferrimagnetic compensation is therefore characterised by an equality of the magnetic sublattices; the reversal of the magnetic structure and a compensated sperimagnetic phase which occurs at exactly T_{comp}.

In **Part II** of this work, the non spin-flip cross-sections, which were also derived from the raw data in absolute units, will be analysed with a Fourier transform. There will be no adjustable parameters in this analysis, other than magnetic moment values which are specified in Sections 2 and 3 above. The results will provide a description of the atomic-scale structures in the two glasses and their variation with temperature in $Fe_{64}Er_{19}B_{17}$.

5) Acknowledgements

The authors would like to thank Dr S Pizzini for her assistance in the measurements of the magnetisation curves of the in $Fe_{64}Er_{19}B_{17}$ glass and Dr J C Criginski for providing information on the x-ray magnetic circular dichroism measurements that he has recently undertaken on the $Fe_{64}Er_{19}B_{17}$ sample. The neutron experiments were made within the EPSRC Neutron Beam programme and the help of the staff at the Institut Laue-Langevin is gratefully acknowledged.

References

[1] Wildes A R and Cowlam N Recent Research Developments in Magnetism and Magnetic Materials 2003 **1** 541-563.

[2] Harris R, Plischke M and Zuckermann M J 1973 Phys Rev Lett **31** 160-2

[3] Sayko G V, Utochkin S N and Zvezdin A K 1992 J Mag and Mag Mat **113** 194-200

[4] Cowlam N, Hanwell M D, Wildes A R and Jenner A G I 2005 J Phys : Condens Matter **17** 3585-3596.

[5] Krishnan R, Lassri H and Teillet J 1991 JMMM **98** 155-61.

[6] Benjelloun J, Baran M, Lassri H, Oukris H, Krishnan R, Omri M and Ayadi M 1999 JMMM **204** 68-72.

[7] García L M, Pizzini S, Rueff J P, Vogel J, Galér, Fontaine A, Kappler J P, Krill G and Goedkoop J B 1996 J Appl Phys **79** 6497-99.

[8] Pizzini S, García L M, Fontaine A, Rueff J P, Vogel J, Galéra R M Goedkoop J B, Brookes N B, Krill G and Kappler J P 1997 J of Elec Spect **86** 165-73

[9] Szymański K, Kalska B, Satuła D, Dobrzyński L, Brodderfalk A, Wäppling R, and Nordblad P 2002 JMMM **251** 271-82.

[10] Hurd C M 1982 Contemp Phys **23** 469-493

[11] Hastings J M and Corliss L M 1962 Phys Rev **126** 556-65

[12] Cowlam N, Wildes A R, Hanwell M D, Dearing N and Jenner A G I 2010 J Phys : Condens Matter **22** 296003-9

[13] Morrish A H 1965 The Physical Principles of Magnetism (John Wiley : New York)

[14] Clegg S J, Purdey J H, Greenhough R D and Jerems F 1994 J Appl Phys **76** 6371-3

[15] Criginski J C, private communication

[16] Brown P J 1995 International Tables for Crystallography
ed Wilson A J C (Dordrech : Kluwer) Vol **C** 391.

[17] Klug H P and Alexander L E 1974 X-ray diffraction procedures (John Wiley : New York)

[18] Cargill G S III 1975 Solid State Physics 30 227-320

[19] http://www.ncnr.nist.gov/resources/n-lengths